Supporting Information

Porous Hollow Manganites with Robust Composite Shells for Oxidation of CO at Low Temperature

Jung Bo Yoo[a], Sora Bang[b], Kyungtae Kim[b], Chengbin Li[c], Ji Man Kim[c] and Nam Hwi Hur[b*]

[a]Nuclear Chemistry Research Division, Korea Atomic Energy Research Institute, 111 Daedeok-daero-989, Yuseong-gu, Daejeon, 34057 Korea

[b]Department of Chemistry, Sogang University, Seoul 121-742, Korea

[c]Department of Chemistry, Sungkyunkwan University, Suwon, 16419, Korea.

*E-mail: nhhur@sogang.ac.kr

I. Experimental

Synthesis of hollow nickel-coated silica microspheres ($Ni@SiO_2$)

The prepared core/shell SiO_2 microspheres (0.495 g) were dispersed in 250 mL of deionized water in a 500 mL round-bottom flask. Nickel acetylacetonate (0.4 g, 1.6×10^{-3} mol) and urea (4.0 g, 6.7×10^{-2} mol) were dissolved into the solution, which was then stirred at 80 ^{o}C for 2 h. The white microspheres gradually became green colloidal spheres, which were separated from the solution by centrifugation (3000 rpm), and dried in an oven at 100 ^{o}C. The dried microspheres ($Ni(OH)_2@SiO_2$) were annealed at 750 ^{o}C for 20 h under a reducing atmosphere (Ar/H_2 = 95:5) to yield the desired nickel-coated microspheres($Ni@SiO_2$). Furthermore, the resultant green colloidal spheres were annealed in air at 700 ^{o}C for 10 h, yielding nickel oxide-coated silica microspheres, which were denoted as $NiO@SiO_2$.

II. Figures

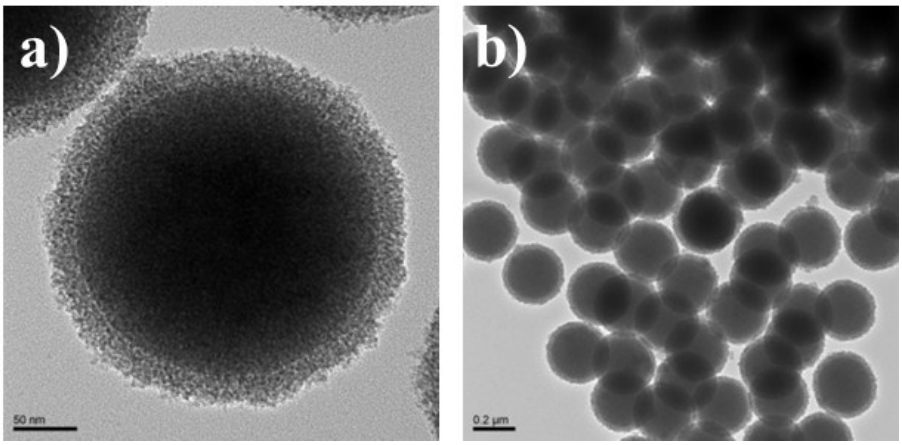

Fig. S1 Representative TEM images of SiO_2 microspheres with a core/shell structure. High and low resolution images are given in a) and b), respectively. The core having a dark image had a diameter of approximately 250 nm and the shell with a bright image had a thickness of 35–45 nm. Both core and shell are composed of Si and O, which was determined by Energy-dispersive X-ray spectroscopy. Carbon residues were not detected.

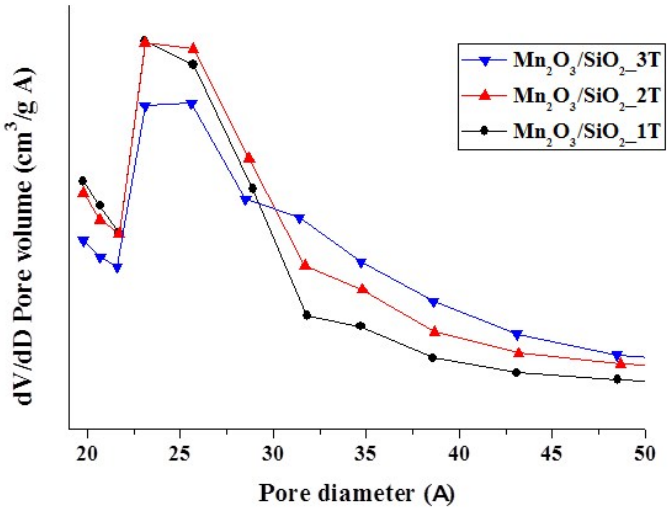

Fig. S2 Pore-size distribution curves of Mn_2O_3/SiO_2_1T, Mn_2O_3/SiO_2_2T, (c) Mn_2O_3/SiO_2_3T, in which pore-size distributions were calculated using the Barrett-Joyner-Halenda method.

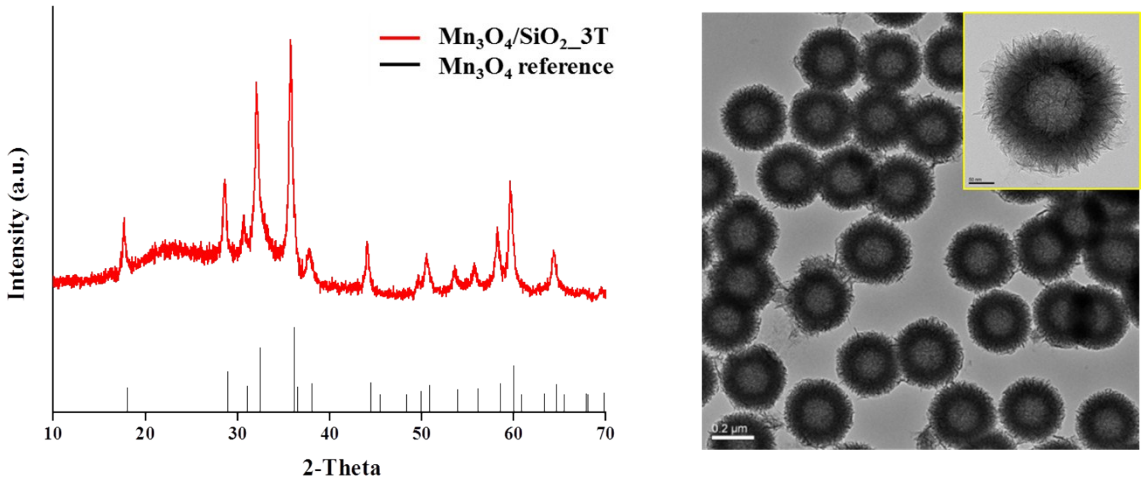

Fig. S3 (a) Powder XRD pattern and (b) representative TEM image of Mn_3O_4/SiO_2_3T microspheres.

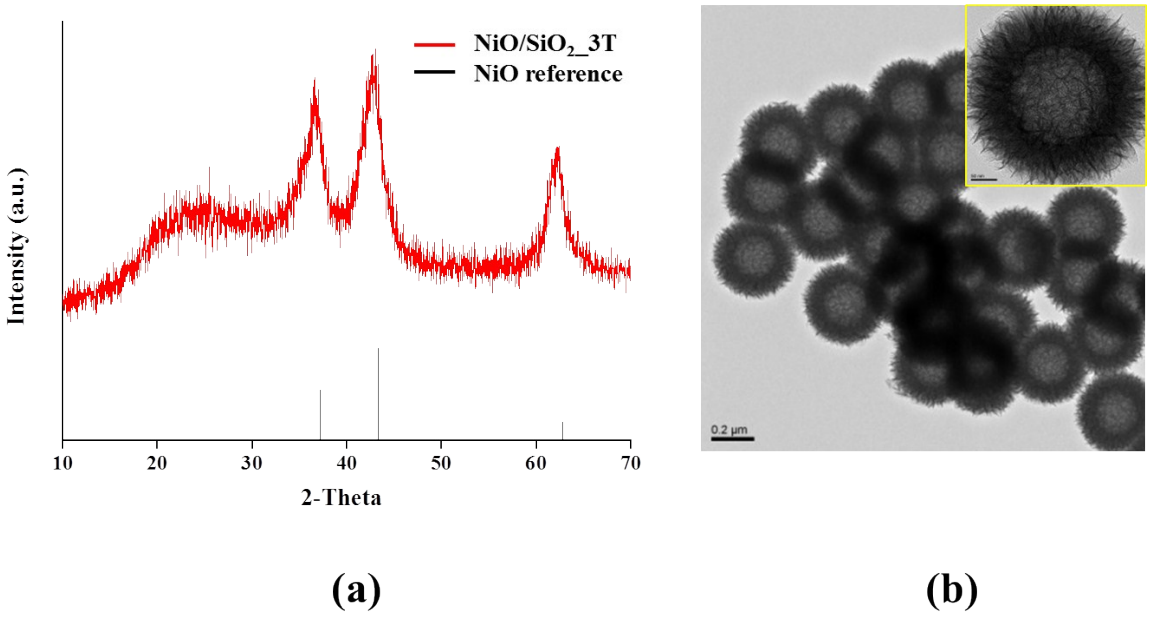

Fig. S4 (a) Powder XRD pattern and (b) representative TEM image of NiO/SiO_2_3T microspheres.

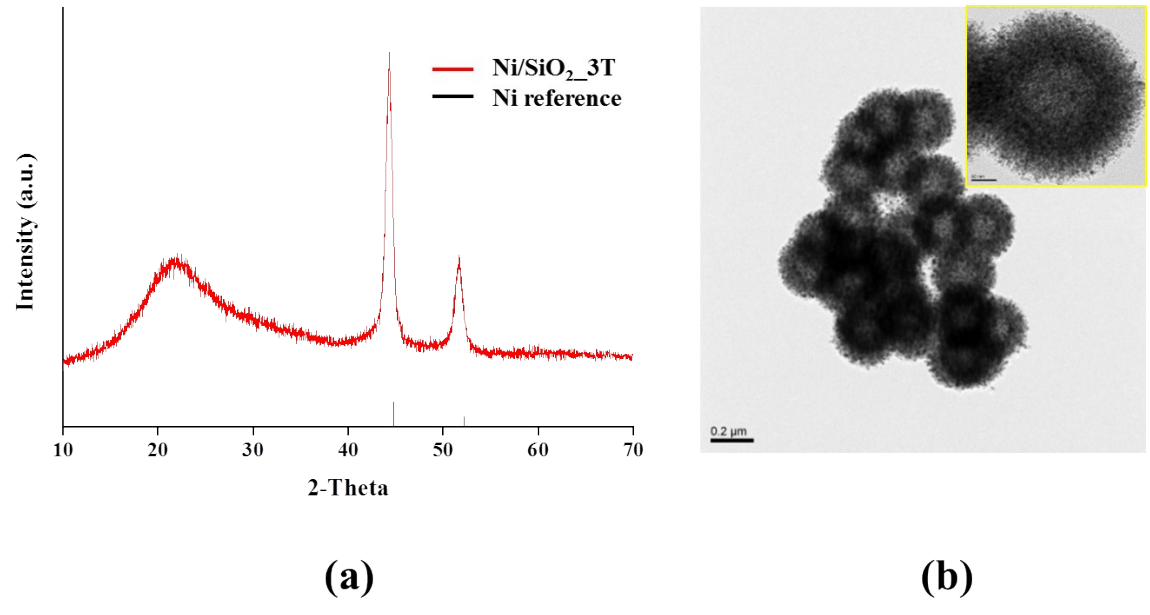

Fig. S5 (a) Powder XRD pattern and (b) representative TEM image of Ni/SiO_2_3T microspheres.

III. Tables

Table S1. Comparison of catalytic performance for CO oxidation of Mn_2O_3/SiO_2_3T with other Mn-based catalysts.

No	Catalysts	S_{BET} [m^2/g]	Conditions	T_{50} [°C]	T_{100} [°C]	Ref	Remark
1	Mn_2O_3/SiO_2_3T	497.11	0.05 g of catalyst, 3.5 % CO and 8.4 % O_2, 50 mL/min	110	< 200	This work	Mn (45.48 wt%)
2	PdO_x/Mn_2O_3	25.50	1 g of catalyst, 2000 ppm CO in air, GHSV = 12200 h^{-1}	130	200	1	PdO_x (1 wt%)
3	Mn_2O_3	37.00	0.05 g of catalyst, 1 % CO, 20 % O_2, 50 mL/min	135	400	2	Mn (53.39 wt%)
4	Au/Mn_2O_3	29.00	0.05 g of catalyst, 1 % CO, 20 % O_2, 50 mL/min	25	100	2	Au (2.9 wt%)
5	Mn_2O_3	20.00	1 mL of catalyst, 1% CO, 18 % O_2, GHSV = 10000 h^{-1}	150	220	3	Mn (53.39 wt%)
6	Mn_2O_3-Al_2O_3	127.04	0.3 g of catalyst, 1 % CO, 18.8 % O_2, 100 mL/min	280	> 300	10	-
7	Au/Mn_2O_3-Al_2O_3	210.12	0.3 g of catalyst, 1 % CO, 18.8 % O_2, 100 mL/min	270	> 300	10	Au (2 wt%)
8	α-Mn_2O_3	37.00	0.05 g of catalyst, 1 % CO, 20 % O_2, 50 mL/min	134	180	5	Mn (53.39 wt%)
9	Mn_2O_3/Mn_3O_4	18.00	0.2 g of catalyst, 5 % CO, 10 % O_2, GHSV = 36000 h^{-1}	300	500	6	Mn (64.59 wt%)
10	3DOM Mn_2O_3	37.70	1% CO, 20 % O_2, GHSV = 20000 h^{-1}	168	> 300	7	Mn (53.39 wt%)
11	α-Mn_2O_3	27.00	1 % CO, 20 % O_2, GHSV = 36000 h^{-1}	155	300	8	Mn (53.39 wt%)
12	Mn_2O_3	-	0.5 g of catalyst, 1:1 mixture CO+O_2, 30 mL/min	210	300	9	Mn (53.39 wt%)
13	Mn_2O_3+SnO_2	-	0.5 g of catalyst, 1:1 mixture CO+O_2, 30 mL/min	120	> 400	9	-
14	γ-Mn_2O_3	-	0.15 g of catalyst, 2.4 % CO, 1.2 % O_2, 80 mL/min	165	> 350	4	Mn (53.39 wt%)
15	Ag/γ-Mn_2O_3	-	0.15 g of catalyst, 2.4 % CO, 1.2 % O_2, 80 mL/min	110	200	4	Ag (20 wt%)
16	Mn_2O_3/SBA-15	226.00	5 % CO, 5 % O_2, GHSV = 6000 h^{-1}	200	> 250	11	-
17	α-Mn_2O_3	-	1 % CO, 20 % O_2, GHSV = 36000 h^{-1}	160	300	12	Mn (53.39 wt%)
18	$Mn_{1.95}Pd_{0.05}O_3$	11.30	0.9 g of catalyst, 5 % CO, 5 % O_2, 80 mL/min	169	190	13	Pd (3.3 wt%)
19	$Mn_{1.92}Pd_{0.08}O_3$	13.50	0.9 g of catalyst, 5 % CO, 5 % O_2, 80 mL/min	160	180	13	Pd (5.3 wt%)

Table S2. Comparison of catalytic performance for CO oxidation of Mn_2O_3/SiO_2_3T with inexpensive catalysts on the basis of metal oxides.

No	Catalysts	Catalyst Weight (mg)	CO Concentration (%)	Flow Rate (mL/min)	T_{50} (°C)	T_{100} (°C)	Ref
1	Mn_2O_3/SiO_2_3T	50	3.5	50.0	110	< 200	This Work
2	$CuO/Ce_{0.8}Zr_{0.2}O_2$	200	10.0	36.6	-	90	14
3	$CuO\text{-}Fe_2O_3$	200	10.0	36.6	-	115	15
4	CuO/MTPs[a)]	200	10.0	36.6	-	300	16
5	CuO/Al_2O_3	150	2.0	100.0	226	> 265	17
6	CuO nanorods	80	15.0	15.0	140	160	18
7	CuO/ARM-20%[b)]	200	10.0	50.0	120	170	19
8	CuO/CeO_2	100	1.0	66.7	100	150	20
9	FeCo15[c)]	200	10.0	36.6	180	250	21
10	LFO-2[d)]	200	1.0	100.0	170	208	22
11	$CuO\text{-}Ce_{1-x}La_xO_{2-x}$	400	5.4	215.0	150	> 300	23

[a)] MTPs: mesoporous titanium phosphonate spheres, [b)] ARM-20%: activated red mud, [c)] FeCo15: mesoporous Co-Fe-O nanocatalysts (FeCo*x*, *x*= Co/Co+Fe), [d)] LFO-2: $LaFeO_3$ (SiO_2 nanospheres as the hard template).

IV. References

1. J. S. Park, D. S. Doh and K. Lee, *Top. Catal*., 2000, **10**, 127.
2. L. Wang, Q. Liu, X. Huang, Y. Liu, Y. Cao and K. Fan, *Appl. Catal. B: Environ*., 2009, **88**, 204.
3. S. Imamura, H. Sawada, K. Uemura and S. Ishida, *J. Catal*., 1988, **109**, 198.
4. R. Lin, W. Liu, Y. Zhong and M. Luo, *Appl. Catal. A: Gen*., 2001, **220**, 165.
5. L. Wang, X. Huang, Q. Liu, Y. Liu, Y. Cao, H. He, K. Fan and J. Zhuang, *J. Catal*., 2008, **259**, 66.
6. S. A. C. Carabineiro, S. S. T. Bastos, J. J. M. órfão, M. F. R. Pereira, J. J. Delgado and J. L. Figueiredo, *Catal. Lett*., 2010, **134**, 217.
7. S. Xie, H. Dai, J. Deng, H. Yang, W. Han, H. Arandiyan and G. Guo, *J. Hazard.*

Mater., 2014, **279**, 392.

8. Y. Luo, Y. Deng, W. Mao, X. Yang, K. Zhu, J. Xu and Y. Han, *J. Phys. Chem. C*., 2012, **116**, 20975.
9. S. K. Kulshreshtha and M. M. Gadgil, *Appl. Catal. B: Environ*., 1997, **11**, 291.
10. B. Malecka and M. Rajska, *Ceram. Mater.,* 2010, **62**, 540.
11. Y. Han, F. Chen, Z. Zhong, K. Ramesh, L. Chen and E. Widjaja, *J. Phys. Chem. B*., 2006, **110**, 24450.
12. J. Xu, Y. Deng, Y. Luo, W. Mao, X. Yang and Y. Han, *J. Catal*., 2013, **300**, 225.
13. R. K. Kunkalekar and A. V. Salker, *Reac. Kinet. Mech. Cat*., 2012, **106**, 395.
14. J-L. Cao, Y. Wang, T-Y. Zhang, S-H Wu and Z-Y. Yuan, *Appl. Catal. B: Environ.,* 2008, **78**, 120.
15. J-L. Cao, Y. Wang, X-L. Yu, S-R. Wang, S-H. Wu and Z-Y. Yuan, *Appl. Catal. B: Environ.,* 2008, **79**, 26.
16. T-Y. Ma and Z-Y. Yuan, *Dalton Trans.,* 2010, **39**, 9570.
17. Z. Boukha, J. L. Ayastuy, A. I-Gonzalez, B. P-Ayo, M. A. G-Ortiz and J. R. G-Velasco, *Appl. Catal. B: Environ.,* 2014, **160**, 629.
18. K. Zhong, J. Xue, Y. Mao, C. Wang, T. Zhai, P. Liu, X. Xia, H. Li and Y. Tong, *RSC Advances,* 2012, **2**, 11520.
19. Z-P. Hu, Y-P. Zhu, Z-M. Gao, G. Wang, Y. Liu, X. Liu and Z-Y. Yuan, *Chem. Eng. J.,* 2016, **302**, 23.
20. S. Zeng, K. Liu, L. Zhang, B. Qin, T. Chen, Y. Yin and H. Su, *J. Power Sources*, **2014**, 261, 46.
21. J-L. Cao, G-J. Li, Y. Wang, G. Sun, X-D. Wang, B. Hari and Z-Y. Zhang, *J. Environ. Chem. Eng.*, 2014, **2**, 477.
22. B. Gao, J. Deng, Y. Liu, Z. Zhao, X. Li, Y. Wang and H. Dai, *Chin. J. Catal.,* 2013, **34**, 2223.

23. J. S. Moura, J. S. L. Fonseca, N. Bion, F. Epron, T. F. Silva, C. G. Maciel, J. M. Assaf and M. C. Rangel, *Catal. Today*, 2014, **228**, 40.